

# Chirally enhanced corrections to FCNC processes in the generic MSSM

Andreas Crivellin and Ulrich Nierste

*Institut für Theoretische Teilchenphysik  
Karlsruhe Institute of Technology, Universität Karlsruhe,  
76128 Karlsruhe, Germany*

## Abstract

Chirally enhanced supersymmetric QCD corrections to FCNC processes are investigated in the framework of the MSSM with generic sources of flavor violation. These corrections arise from flavor-changing self-energy diagrams and can be absorbed into a finite renormalization of the squark-quark-gluino vertex. In this way enhanced two-loop and even three-loop diagrams can be efficiently included into a leading-order (LO) calculation. Our corrections substantially change the values of the parameters  $\delta_{23}^{dLL}$ ,  $\delta_{23}^{dLR}$ ,  $\delta_{23}^{dRL}$ , and  $\delta_{23}^{dRR}$  extracted from  $\text{Br}[B \rightarrow X_s \gamma]$  if  $\tan \beta$  is large. We find stronger (weaker) constraints compared to the LO result for negative (positive) values of  $\mu$ . The constraints on  $\delta_{13}^{dLR,RL}$  and  $\delta_{23}^{dLR,RL}$  from  $B_d - \bar{B}_d$  and  $B_s - \bar{B}_s$  mixing change drastically if the third-generation squark masses differ from those of the first two generations.  $K - \bar{K}$  mixing is more strongly affected by the chirally enhanced loop diagrams and even sub-percent deviations from degenerate down and strange squark masses lead to profoundly stronger constraints on  $\delta_{12}^{dLR,RL}$ .

## 1 Introduction

Processes involving Flavor-Changing Neutral Currents (FCNCs) are of great importance for supersymmetric model building, because they probe the supersymmetry-breaking sector with an enormous sensitivity. In the Minimal Supersymmetric Standard Model (MSSM) with generic flavor structure FCNC processes are mediated by the strong interaction through diagrams involving squarks and gluinos. Today's precise experimental data on flavor violation in K, D and B physics leave little room for mechanisms of flavor violation other than the established Cabibbo-Kobayashi-Maskawa mechanism of the Standard Model (SM). This incompatibility of the generic MSSM with experiment is known as the SUSY flavor problem. It points towards a mechanism of supersymmetry breaking which is dominantly flavor-blind and only feels the flavor violation of the Yukawa sector. From a phenomenological point of view one would like to assess the possible size of the deviations from this scenario of *minimal flavor violation* (MFV). In an appropriately chosen basis of the (s)quark superfields (the super-CKM basis) one can parameterize the deviations from MFV by flavor-off-diagonal entries of the squark mass matrices. By confronting the squark-gluino mediated amplitudes with precision data one can constrain the sizes of these off-diagonal squark-mass terms. Once superparticles are discovered and their masses are determined, these FCNC analyses may lead to insights into the mechanism of supersymmetry breaking.

When the MSSM with explicit soft breaking was first written down in [1] it was already realized, that these breaking-terms are potential sources of flavour violation. Elaborating further on this topic,

Ref. [2–5] discovered that neutralinos and gluinos have flavor-changing couplings once the quark and squark fields are rotated into the physical basis with diagonal mass matrices. In order to simplify the calculations and to parameterize the non-minimal sources of flavor violation in a generic way the mass insertion approximation (MIA) was invented [6]. MIA amounts to an expansion in the small flavor-changing squark mass terms to lowest non-vanishing order. Later the authors of Ref. [7, 8] studied FCNCs with non-minimal sources of flavor violation in the context of various supersymmetric grand unified theories. In Ref. [9] an explicit calculation of the gluino boxes contributing to  $\Delta F = 2$  processes and a matching to the effective Hamiltonian of flavor physics was carried out for the first time, using both MIA and the exact diagonalization of the squark mass matrices. In the seminal 1996 paper of Gabbiani et. al. [10] FCNC data (on B mixing, K mixing,  $\mu \rightarrow e\gamma$  and  $b \rightarrow s\gamma$ ) were used to constrain the off-diagonal elements of the sfermion mass matrices, while the diagonal ones were constrained from the electric dipole moments (and from a fine tuning argument). In that work the mass insertion approximation was used and QCD corrections were briefly discussed. After the QCD corrections to the full  $\Delta F = 2$  Hamiltonian were calculated at leading order (LO) [11] and next-to-leading order (NLO) [12] an improved calculation of Kaon mixing in the generic MSSM has lead to more accurate bounds on the off-diagonal elements of the squark mass matrix [11, 13]. In 1999 an extensive study of  $b \rightarrow s\gamma$  with LO Wilson coefficients [14] was performed. Ref. [15] extended the study of Ref. [14] by including the MFV effects. Ref. [16] has addressed B mixing at NLO, Ref. [17, 18] contains an update of the constraints from  $b \rightarrow s$  transitions and Ref. [19] has discussed D mixing. In the meantime also the Wilson coefficients for  $\Delta F = 2$  processes have been calculated at NLO [20]. The importance of chirally-enhanced beyond-LO corrections in the generic MSSM was discussed in a series of articles by Foster et al. [21]. Recently, constraints on the off-diagonal elements of the squark mass matrix have been obtained from a fine-tuning argument applied to the renormalization of the Cabibbo-Kobayashi-Maskawa (CKM) matrix [22] and from a loop-induced effective right-handed W coupling [23].

Large FCNC effects with a different phenomenological pattern can be expected if the squark mass matrices contain large chirality-flipping but flavor-conserving entries. This situation occurs if the ratio  $\tan \beta = v_u/v_d$  of the Higgs vevs is large and can be traced back to an effective loop-induced coupling of the Higgs doublet  $H_u$  to down-type quarks  $d_j$ , where  $j = 1, 2, 3$  labels the fermion generation [24]. Hall, Rattazzi and Sarid discovered the relevance of this loop contribution for large- $\tan \beta$  phenomenology [25] and the authors of Ref. [26] observed that  $\tan \beta$ -enhanced loop-induced FCNC Higgs couplings occur even in MFV scenarios. If the chirality violation is proportional to a Yukawa coupling further a resummation of the enhanced loops to all orders in perturbation theory is necessary. This resummation can be achieved analytically with the help of an effective two-Higgs-doublet Lagrangian (valid in the decoupling limit of infinite sparticle masses) [26, 27] or through an explicit diagrammatic resummation [28–30]. In the diagrammatic method the enhanced loop effects occur through chirality-flipping self-energies which are chirally enhanced by a factor of  $\tan \beta$ .

In this paper we study the effects of chirally-enhanced flavor-changing self-energies in the generic MSSM. The first possibility for a chiral enhancement factor is  $A_{ij}^d v_d / (M_{\text{SUSY}} \text{Max}[m_{d_i}, m_{d_j}])$  with a flavor-changing trilinear SUSY-breaking term  $A_{ij}^d$  dominating over a small quark mass  $m_{d_{i,j}}$  in the denominator.  $M_{\text{SUSY}}$  is the mass scale determining the size of the loop diagram, i.e.  $M_{\text{SUSY}}$  is roughly the maximum of the gluino and squark masses running in the loop. The second possible chiral enhancement factor is  $(v/M_{\text{SUSY}}) \tan \beta$  accompanied by a flavor-changing squark mass term involving squark fields of the same chirality. These self-energies have been analyzed in the context of charged-current processes in Ref. [22] and this paper contains the complementary study of FCNC processes. As an example, consider  $B_s - \bar{B}_s$  mixing, with the LO diagrams shown in Fig. 1. In

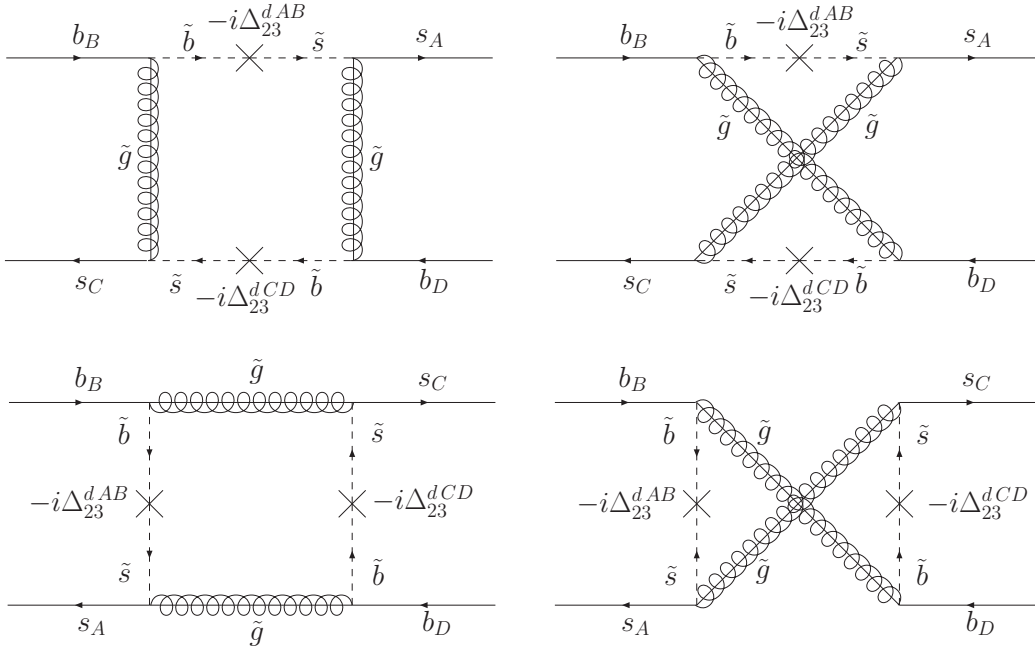


Figure 1: One-loop gluino squark diagrams contributing to  $B_s - \bar{B}_s$  mixing in the presence of flavor-off-diagonal  $A^d$  terms. The crosses denote mass insertions while  $A, B, C$  and  $D$  label the chiralities (equal to  $L$  or  $R$ ) with  $A \neq B$  and  $C \neq D$ .

the presence of chirally enhanced corrections one must also take into account two- or even tree-loop diagrams, because the loop suppression is offset by the chiral enhancement factor (see Fig. 2). Similar corrections have been considered before in Ref. [21]. However, the authors of these papers have used a different definitions of the super-CKM basis and of the parameters  $\delta_{fi}^{qAB}$  describing the flavour violation in the squark mass matrices. As a consequence, our results are hardly comparable to the ones obtained in Ref. [21]. We elaborate on the differences between Ref. [21] and this paper in Sect. 2. We note that models in which CKM elements and light-fermion masses are generated radiatively [22, 31] require large trilinear SUSY-breaking terms. In the presence of these large  $A$ -terms (or of a large factor of  $m_b \mu \tan \beta$  in combination with chirality-conserving flavor violation) it is important to include the effect of the chirality-flipping self-energies into FCNC processes. We will accomplish this in Sect. 2 by renormalizing the quark-squark-gluino vertex by a matrix-valued quark-field rotation in flavor space. In Sect. 3 the radiative decay  $b \rightarrow s \gamma$  is examined in detail. The chirally enhanced corrections are only relevant for the large- $\tan \beta$  case here (or if  $v_d A_{33}^d$  large). In Sect. 4,  $\Delta F = 2$  processes are investigated, where large corrections occur irrespective of the size of  $\tan \beta$  if the flavor violation is due to  $A$ -terms and if the squarks are not degenerate. Up-to-date measurements and theoretical Standard-Model predictions are used. The theoretical uncertainties of the SM are treated in a consistent and systematic way. In each case we compare the size of the FCNC transition to the previously known LO result: With the inclusion of our self-energies the bounds on the off-diagonal elements of the squark mass matrix change drastically, especially if the SUSY particles are rather heavy. In Sect. 5 we conclude.

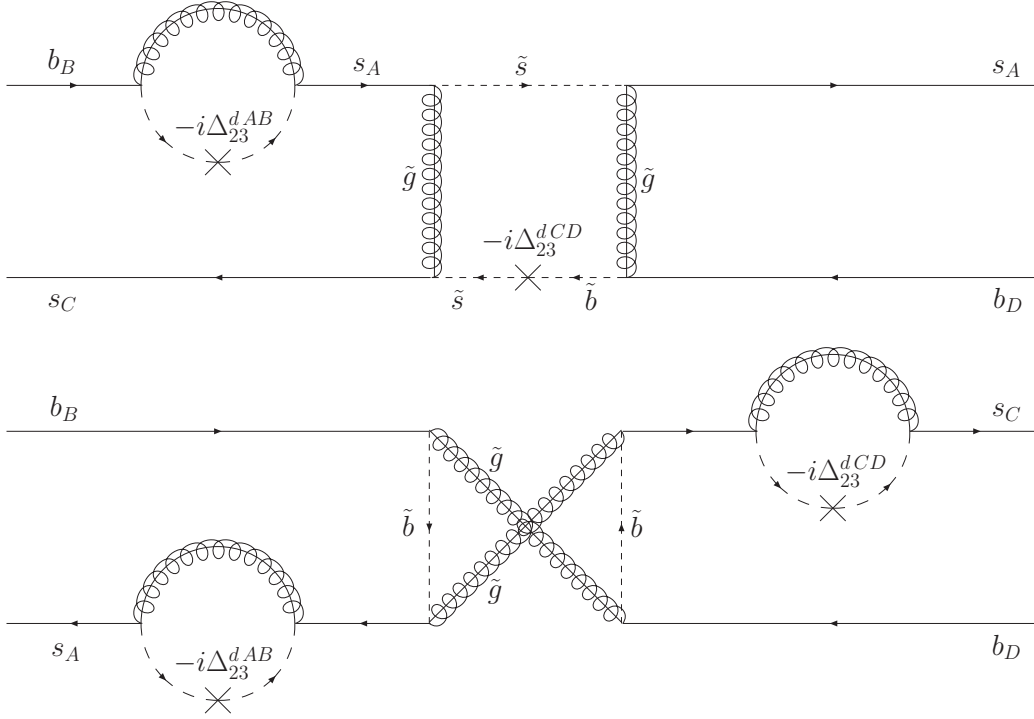


Figure 2: Examples of two-loop and three-loop diagrams which can compete with (or even dominate over) the one-loop diagrams in Fig. 1.

## 2 One-loop renormalization of the quark-squark-gluino vertex

In this section we show how to treat the chirally enhanced parts of flavor-changing self-energies in the full MSSM and how to absorb them into mixing matrices entering the Feynman rule of the quark-squark-gluino vertex. In this way all enhanced two-loop and three-loop diagrams are automatically included in the LO calculation to all orders in  $v/M_{\text{SUSY}}$ .

Chirally enhanced corrections, in which we are interested here, have been calculated in Ref. [21] from a loop-corrected quark mass matrix, in a formalism in which the heavy SUSY particles are integrated out. When these expressions are combined with some one-loop amplitude this method can, in principle, reproduces the chirally enhanced two-loop (or three-loop) FCNC amplitude to leading non-vanishing order in  $v/M_{\text{SUSY}}$ , where  $v = \sqrt{v_u^2 + v_d^2} = 174 \text{ GeV}$  is the electroweak vev. Since the squark mixing angles scale as  $v/M_{\text{SUSY}}$ , scenarios with large left-right mixing among squarks are not properly covered in this approach. In particular, the widely-studied large- $\tan \beta$  scenarios typically involve large sbottom mixing and therefore call for an analysis beyond the decoupling limit. On the other hand, Ref. [21] goes beyond our work by also including electroweak and Higgs-mediated contributions to the Wilson-coefficients. Another important difference between Ref. [21] and this paper concerns the definitions of the super-CKM basis and the mass insertion parameters:

- We use the tree-level definition of the super-CKM basis (see Ref. [22]) which permits an analytical solution to the necessary all-order resummations of enhanced corrections. With the on-shell definition of Ref. [21] the self-energies and the squark mass matrices depend mutually on each

other, which requires an iterative numerical evaluation of both quantities. This definition clouds the relations between observables and fundamental parameters like the trilinear SUSY-breaking terms  $A_{fi}^{u,d}$  (as discussed later in this section). Our results are more transparent and enable us to identify a previously neglected parameter region with dramatically enhanced corrections to meson-antimeson mixing (see Sect. 4.)

- Concerning the definition of the mass insertion parameters  $\delta_{fi}^{q AB}$  we choose the most common one (see for example [10, 12–14, 16–20, 22]) in which the mass insertion is the entire off-diagonal element of the squark mass matrix divided by the average squark mass. On the other hand, the authors of Ref. [21] only include the term  $v_q A^q$  into their definition of the mass insertion parameters. This leads to an artificial dependence of all corrections, even the ones independent of a quark mass, on  $\tan \beta$ . Furthermore, if the authors of Ref. [21] would have chosen our definition of the mass insertions (while keeping their definition of the super-CKM basis) all chirally enhanced corrections would be simply absent, instead they would be implicitly contained in the definition of the  $\delta_{fi}^{q AB}$ s.

Throughout this paper we use the notations and conventions of Ref. [22]. The self-energies can be divided into a chirality-flipping and a chirality-conserving part:

$$\Sigma_{fi}^q(p) = \Sigma_{fi}^{q RL}(p^2) P_L + \Sigma_{fi}^{q LR}(p^2) P_R + \not{p} \left[ \Sigma_{fi}^{q LL}(p^2) P_L + \Sigma_{fi}^{q RR}(p^2) P_R \right] \quad (1)$$

Since the SUSY particles are known to be much heavier than the five lightest quarks, it is possible to expand in the external momentum unless one external quark is the top. We are not going to study the case of an external top further in this article, because there are no useful data on FCNC top decays. The part proportional to  $\not{p}$  in Eq. (1) can be neglected since no chiral enhancement is possible. Thus the following simplified expression for the self-energy is sufficient for our purpose:

$$\Sigma_{fi}^{q RL, LR}(p^2 = 0) = \frac{2m_{\tilde{g}}}{3\pi} \alpha_s(M_{\text{SUSY}}) \sum_{s=1}^6 V_{s fi}^{(0) q RL, LR} B_0(m_{\tilde{g}}, m_{\tilde{q}_s}), \quad (2)$$

If  $v_q A_{fi}^q$  is large, FCNC diagrams with this self-energy in an external leg (as in Fig. 2) will compete with the leading order diagram (see Fig. 1). For  $q = d$  the enhancement can further stem from  $m_b \mu \tan \beta$  in which case an all-order resummation is necessary [28, 30], leading to a correction of the tree-level relation  $m_{d_i} = v_d Y^{d_i}$  to

$$Y^{d_i} = \frac{m_{d_i}}{v_d (1 + \Delta_{d_i})} = \frac{m_{d_i} - \Sigma_{ii, A}^{d LR}}{v_d + \Sigma_{ii, \mu}^{d LR} / Y^{d_i}}. \quad (3)$$

In Eq. (3) we have used the fact that  $\Sigma_{ii}^{d LR}$  can be decomposed into  $\Sigma_{ii, A}^{d LR} + \Sigma_{ii, \mu}^{d LR}$  even if the physical squark masses are chosen as input parameters.  $\Sigma_{ii, \mu}^{d LR}$  is proportional to  $\mu Y_{d_i}$  (and  $\Sigma_{ii, \mu}^{d LR} / Y^{d_i}$  is independent of  $Y^{d_i}$ ) and  $\Sigma_{ii, A}^{d LR}$  is proportional to  $A_{ii}^d$ . If we neglect the latter contribution Eq. (3) reduces to the expression of Ref. [28].  $m_{d_i}$  is the physical quark mass, with an on-shell subtraction of the SUSY contributions, as determined from low-energy data. For a detailed discussion of the relation between Yukawa couplings and quark masses for different renormalization schemes see Ref. [30]. For up-quarks one must replace  $d \rightarrow u$  in Eq. (3) and may omit  $\Sigma_{ii, \mu}^{d LR}$ , which is now suppressed with  $\cot \beta$ .

As already mentioned, the chirally enhanced parts of the SQCD self-energies do not decouple. This means they do not vanish in the limit  $M_{\text{SUSY}} \rightarrow \infty$  but rather converge to a constant. Therefore the

corresponding FCNC diagrams of the type in Fig. 1 scale with  $M_{\text{SUSY}}$  in the same way as the LO diagram. We will find that the two-loop and three-loop diagrams compete with the LO ones, especially for rather large and non-degenerate squark masses. There are different possibilities to handle flavor-changing self-energies in external legs: The conceptually simplest version is to treat them in the same way as one-particle-irreducible diagrams [32]. So far we have implied this method, which is best suited to identify chirally enhanced contributions. Calculations are easiest, however, if one absorbs the chirally enhanced corrections into the quark-squark-gluino vertex through unitary rotations  $\Delta U_A^q$  ( $A = L, R$  denotes the chirality) in flavor space [22]. These rotations alter the Feynman rule for the squark-quark-gluino vertex:

$$\begin{aligned} W_{s,i}^{q*} &\rightarrow W_{s,j}^{q*} \left(1 + \Delta U_{L\,ji}^q\right) \\ W_{s,i+3}^{q*} &\rightarrow W_{s,j+3}^{q*} \left(1 + \Delta U_{R\,ji}^q\right) \end{aligned} \quad (4)$$

with

$$\begin{aligned} \Delta U_L^q &= \begin{pmatrix} 0 & \frac{1}{m_{q_2}} \Sigma_{12}^{q\,LR} & \frac{1}{m_{q_3}} \Sigma_{13}^{q\,LR} \\ \frac{-1}{m_{q_2}} \Sigma_{21}^{q\,RL} & 0 & \frac{1}{m_{q_3}} \Sigma_{23}^{q\,LR} \\ \frac{-1}{m_{q_3}} \Sigma_{31}^{q\,RL} & \frac{-1}{m_{q_3}} \Sigma_{32}^{q\,RL} & 0 \end{pmatrix} \\ \Delta U_R^q &= \begin{pmatrix} 0 & \frac{1}{m_{q_2}} \Sigma_{12}^{q\,RL} & \frac{1}{m_{q_3}} \Sigma_{13}^{q\,RL} \\ \frac{-1}{m_{q_2}} \Sigma_{21}^{q\,LR} & 0 & \frac{1}{m_{q_3}} \Sigma_{23}^{q\,RL} \\ \frac{-1}{m_{q_3}} \Sigma_{31}^{q\,LR} & \frac{-1}{m_{q_3}} \Sigma_{32}^{q\,LR} & 0 \end{pmatrix} \end{aligned} \quad (5)$$

The procedure in Eq. (4) can be viewed as a short-cut to include the self-energy in the external quark line, in the spirit of Ref. [32]. Alternatively Eq. (4) can be interpreted as a finite matrix-valued renormalization of the quark fields which cancels the external self-energies and reappears in the Feynman rule of the quark-squark-gluino vertex.<sup>1</sup> The inclusion of the enhanced corrections into the LO calculation is now simply achieved by performing the replacements of Eq. (4) in this Feynman rule. Therefore here the exact diagonalization of the squark mass matrix is preferred over MIA. The exact diagonalization has also the advantage that the analysis can be extended to the large  $\tan \beta$  region in which certain off-diagonal entries can have the same size as the diagonal ones.

Here a comment on the definition of the super-CKM basis and the renormalization scheme is in order (see also Ref. [22]):

- i) We define the super-CKM basis as follows: Starting from some weak basis we diagonalize the tree-level Yukawa couplings and apply this unitary transformation to the whole supermultiplet. This is a natural definition of the super-CKM basis because of the direct correspondence between the SUSY-breaking Lagrangian and physical observables. Whenever we refer to some element of a squark mass matrix, this element is defined in this basis. When passing from LO

---

<sup>1</sup>We stress that we do not introduce ad-hoc counter-terms to the quark-squark-gluino vertex. Supersymmetry links the renormalization of the latter to the quark-quark-gluon vertex (which is unaffected by the rotations in Eq. (5)) and the renormalization of the soft SUSY-breaking terms (which can feed into the renormalization of the squark rotation matrices). The requirement to maintain the structure of a softly broken SUSY theory within the renormalization process restricts the allowed counterterms to the quark-squark-gluino vertex. Counterterms stemming from field renormalizations, however, are harmless in this respect, because field renormalizations trivially drop out from the LSZ formula for transition matrix elements.



to NLO or even higher orders the definition of the squark mass matrices is unchanged, i.e. no large chirally enhanced rotations appear at this step. Any additional non-enhanced (i.e. ordinary SQCD) corrections are understood to be renormalized in a way which amounts to a minimal renormalization of the squark mass matrices.

- ii) From given squark mass matrices we calculate the self-energies  $\Sigma_{fi}^{qRL}$  and then the rotations  $\Delta U_{L,R}^q$  in Eq. (4). Calculating LO amplitudes with the corrected  $W_{sk}^{q*}$  from Eq. (4) then properly includes the desired chirally enhanced effects. The order of the two steps is important: First the super-CKM basis is defined from the tree-level structure of the Yukawa sector and the finite loop effects are included afterward, without influence on the definition of the super-CKM basis.

Alternatively one could define the super-CKM basis using an on-shell scheme which eliminates the self-energies in the external legs by shifting their effect into the definition of the super-CKM basis: Applying the inverse of the rotation in Eq. (4) first to the whole (s)quark superfields will leave the squark-quark-gluino vertex flavor-diagonal. (Further supersymmetry is still manifest, e.g. the sbottom field is the superpartner of the bottom field. This would not be the case if different rotations were applied to quark and squark fields.) If one defines this basis as the super-CKM basis (which now changes in every order of perturbation theory) one will find very different constraints on the off-diagonal elements of the squark mass matrices than with our method. The effect of the enhanced self-energies will be entirely absorbed into the values of the elements of the squark mass matrices, these self-energies will not appear explicitly, and the calculation of LO diagrams in the usual way will be sufficient. However, the squark mass matrices determined from data using this method will not be simply related to a mechanism of SUSY breaking, because the extracted numerical value of a given matrix element will also contain the physics associated with the chirally enhanced self-energies. Effects from SUSY breaking and electroweak breaking are interwoven now and further the elements of the squark mass matrix do not obey simple RG equations anymore.

It is illustrative to consider the popular case of soft-breaking terms which are universal at a high scale, say, the GUT scale. The unitary rotations diagonalizing the Yukawa couplings will lead to soft-breaking terms which are proportional to the unit matrix in flavor space. The RG evolution down to low scales will then lead to small flavor-off-diagonal LL entries of the squark mass matrices which are governed by the tree-level (as defined in Ref. [22]) CKM matrix. Obviously, the elements of the squark mass matrices defined in this way are the quantities which one wants to probe in order to discriminate between high-scale universality and other possible mechanisms of soft flavor violation. The above-mentioned unitary rotations diagonalize the tree-level Yukawa couplings, while the rotations with  $\Delta U_{L,R}^q$  are only meaningful after electroweak symmetry breaking and are therefore a low-scale phenomenon. During the RG evolution the Yukawa couplings essentially stay diagonal and the small unitary rotations bringing the low-scale Yukawa couplings back to diagonal form are unrelated to the soft breaking sector (and involve no chiral enhancement). Therefore the procedure described in items i) and ii) is the adequate method to probe the flavor structure of SUSY breaking. For a discussion of renormalization schemes in the context of MFV see Ref. [33].

Consider an FCNC transition  $d_i \rightarrow d_f$  in MIA: If the squark mass  $m_{\tilde{d}_i}$  is degenerate with  $m_{\tilde{d}_f}$ , the renormalization effects of the squark-quark-gluino vertex drop out in FCNC processes. This can be understood in the diagrammatical approach by realizing that diagrams with a flavor-changing self-energy in the outgoing  $f$  leg cancel with the diagram where the self-energy is in the incoming  $i$  leg, because the intermediate loop is the same for both diagrams. Thus, in order to demonstrate the effects of the renormalized quark-squark-gluino vertex non-degenerate squarks are necessary. For

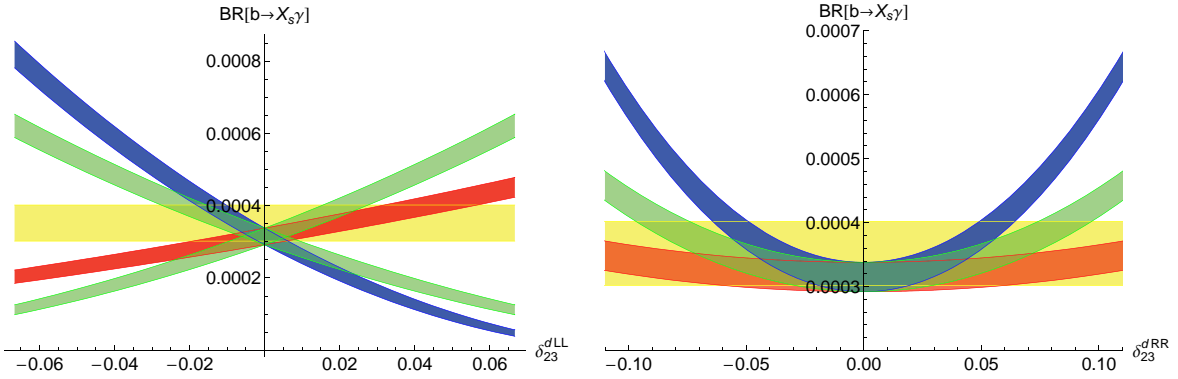


Figure 3:  $\text{Br}[B \rightarrow X_s \gamma]$  as a function of  $\delta_{23}^{dLL}$  and  $\delta_{23}^{dRR}$ , respectively, for  $m_{\tilde{g}} = 750 \text{ GeV}$ ,  $m_{\tilde{q}1/2} = 2m_{\tilde{q}3} = 1000 \text{ GeV}$  and  $\tan \beta = 50$ . Yellow(lightest): experimentally allowed range for  $\text{Br}[B \rightarrow X_s \gamma]$ . Green, red, blue (light to dark): theoretically predicted range for  $\mu/(1 + \Delta_b) = \pm 600 \text{ GeV}$  without renormalization,  $+600 \text{ GeV}$  with renormalized vertices,  $-600 \text{ GeV}$  with renormalized vertices. In the left figure the green band with positive (negative) slope corresponds to the LO branching-ratio with  $\mu/(1 + \Delta_b) = +600 \text{ GeV}$  ( $\mu/(1 + \Delta_b) = -600 \text{ GeV}$ ).

definiteness we choose the flavor-diagonal left-handed and right-handed mass terms equal and further set  $m_{\tilde{q}1, \tilde{q}2} = 2m_{\tilde{q}3}$  if not mentioned otherwise. Lighter third-generation squarks are plausible in scenarios with high-scale flavor universality, in which renormalization group (RG) effects usually drive the bilinear soft terms of the third generation down.

At this point we may compare our results in Eq. (5) with the corresponding expressions in Ref. [21]. Unlike our  $\Delta U_{L,R}^q$  the enhanced corrections in Ref. [21] depend explicitly on  $\tan \beta$ . This feature reflects the different definitions of the  $\delta_{fi}^{qAB}$ 's adopted in the two approaches. In particular, the constraints which we will derive from  $\Delta F = 2$  processes in Sect. 4 are very different from those in Ref. [21].

### 3 $B \rightarrow X_s \gamma$

In this section we examine the radiative decay  $b \rightarrow s \gamma$ . We show how the renormalization of the quark-squark-gluino vertex affects the branching-ratio for different values of  $\mu$ .<sup>2</sup> Throughout this section we assume that  $\mu$  and the elements  $\Delta_{ij}^{qAB}$  with  $AB = LL, LR, RL, RR$ , of the squark mass matrices are real. We consider only the case in which  $|\mu| \tan \beta$  is large, because otherwise our new contributions are suppressed and no new constraints can be found. The reason for this feature is the chirality structure of the magnetic transition mediated by the operator  $O_7$ : Both the flavor-changing self-energy and the now flavor-conserving magnetic loop are necessarily chirality-flipping. The chiral enhancement of the latter is achieved by a large value of  $|\mu| \tan \beta$ . We further recall that the contributions from the dimension-six operators  $O_{7b, \tilde{g}}$  and  $O_{8b, \tilde{g}}$  (defined according to Ref. [14]) are suppressed by a factor of  $\frac{M_{\text{SUSY}}}{\mu \tan \beta}$  compared to the contributions from  $O_{7\tilde{g}}$  and  $O_{8\tilde{g}}$ . Furthermore, since all other SQCD contributions are also suppressed we only need to consider the magnetic operators and their

<sup>2</sup>We find agreement of our LO Wilson coefficients with the gluino part given in Ref. [14, 15].



chromomagnetic counterparts:

$$O_{7\tilde{g}} = eg_s^2(Q) \bar{s} \sigma_{\rho\nu} P_R b F^{\rho\nu}, \quad O_{8\tilde{g}} = g_s^3(Q) \bar{s} \sigma_{\rho\nu} T^a P_R b G^{a\rho\nu} \quad (6)$$

$$\tilde{O}_{7\tilde{g}} = eg_s^2(Q) \bar{s} \sigma_{\rho\nu} P_L b F^{\rho\nu}, \quad \tilde{O}_{8\tilde{g}} = g_s^3(Q) \bar{s} \sigma_{\rho\nu} T^a P_L b G^{a\rho\nu} \quad (7)$$

In [14] the matching scale  $Q$  is chosen as  $Q = M_W$ . We use  $Q = m_t$  instead, because it is closer to the SUSY scale while still permitting 5-flavor running of  $\alpha_s$ . The experimental value of [34] is taken at  $2\sigma$  confidence level. For the theoretical prediction, the value of reference [35] is used at the lower and upper end of the error range. We have not used the cumbersome NNLO formula of Ref. [35], but have instead fitted  $C_{7SM}$  in the simple LO formula to reproduce the numerical NNLO result for  $\Gamma(b \rightarrow s\gamma)$ . The LO expression reads

$$\begin{aligned} \Gamma(b \rightarrow s\gamma) &= \frac{m_b^5 G_F^2 |V_{tb} V_{ts}^*|^2 \alpha}{32\pi^4} \left( |C_7|^2 + |\tilde{C}_7|^2 \right) \\ C_7 &= \frac{-16\sqrt{2}\pi^3 \alpha_s(\mu_b)}{G_F V_{tb} V_{ts}^* m_b} C_{7\tilde{g}} + C_{7SM} \\ \tilde{C}_7 &= \frac{-16\sqrt{2}\pi^3 \alpha_s(\mu_b)}{G_F V_{tb} V_{ts}^* m_b} \tilde{C}_{7\tilde{g}} \end{aligned} \quad (8)$$

To check our approximations we have also calculated the NLO evolution with matching at  $Q = M_{\text{SUSY}}$ , but found only a slightly different result.

We now discuss the dependence of  $b \rightarrow s\gamma$  on the different squark mass parameters  $\Delta_{23}^{dAB}$  (or, equivalently, on the usual dimensionless quantities  $\delta_{23}^{dAB}$ ): If the chirality-conserving elements  $\Delta_{23}^{dLL,RR}$  are the non-minimal source of flavor violation  $b \rightarrow s\gamma$  depends very strongly on  $\mu \tan \beta$  already at the one-loop level (i.e. without the renormalization of the quark-squark-gluino vertex). With the inclusion of the flavor-changing self-energies in the external legs  $C_{7\tilde{g},8\tilde{g}}$  is enhanced (suppressed) if  $\mu$  is negative (positive) compared to the LO coefficient. The size of the effect is rather different for  $\delta_{23}^{dLL}$  and  $\delta_{23}^{dRR}$ , because only in the first case interference with  $C_{7SM}$  is possible (see Fig. 3).

For the chirality-violating elements of the squark mass matrix,  $\Delta_{23}^{dLR,RL}$ , this dependence on  $\mu \tan \beta$  is absent at LO and comes only into the game by the renormalization of the squark-quark-gluino vertex. Again the behavior is different for  $\delta_{23}^{dLR}$  compared to  $\delta_{23}^{dRL}$ , since only in the first case interference with  $C_{7SM}$  is possible (see Fig. 4). As we easily see from Fig. 4 the inclusion of the two-loop effects can substantially change the branching ratio. For positive (negative) values of  $\mu$  the size of the Wilson coefficient  $C_{7\tilde{g}}$  decreases (increases), i.e. the qualitative effect of our corrections is the same as for the LL and RR elements in Fig. 3.

In Fig. 5 we plot the constraints obtained from  $\text{Br}[B \rightarrow X_s \gamma]$  on  $\delta_{23}^{dAB}$  versus  $\mu/(1 + \Delta_b)$  for different values of  $m_{\tilde{g}}$ . ( $\Delta_b = \Delta_{d3}$  is defined in Eq. (3).) All four different chirality combinations are shown. The constraints on  $\delta_{23}^{dLR}$  and  $\delta_{23}^{dLL}$  are stronger than the ones on  $\delta_{23}^{dRL}$  and  $\delta_{23}^{dRR}$  with exception of the "conspiracy" regions where the SUSY contributions overcompensate the SM value for  $C_7$ . For  $\delta_{23}^{dLR,RL}$  the allowed region widens from bottom to top, meaning that negative values of  $\mu$  strengthen the bounds on these quantities while positive values of  $\mu$  weaken them. For  $\delta_{23}^{dLL,RR}$  the effect of  $\mu$  is different, as one can verify from the two lower plots in Fig. 5: The bounds on  $\delta_{23}^{dLL,RR}$  always get stronger for increasing  $|\mu|$  but are more stringent for  $\mu < 0$  than for  $\mu > 0$ .

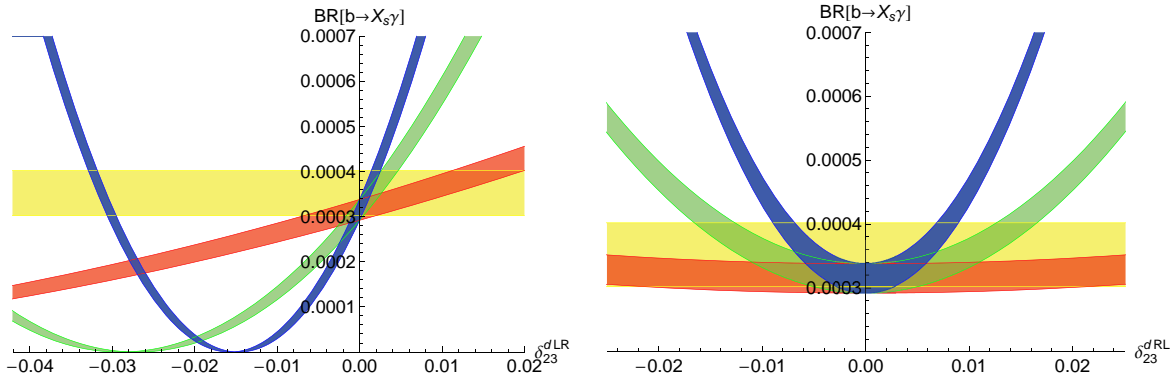


Figure 4:  $\text{Br}[B \rightarrow X_s \gamma]$  as a function of  $\delta_{23}^{dLR}$  and  $\delta_{23}^{dRL}$ , respectively, for  $m_{\tilde{g}} = 750 \text{ GeV}$ ,  $m_{\tilde{q}1, \tilde{q}2} = 2m_{\tilde{q}3} = 1000 \text{ GeV}$ , and  $\tan \beta = 50$ . Yellow(lightest): experimentally allowed range for  $\text{Br}(B \rightarrow X_s \gamma)$ . Green, red, blue (light to dark): theoretically predicted range for  $\mu/(1 + \Delta_b) = 0 \text{ GeV}$ ,  $\mu/(1 + \Delta_b) = 600 \text{ GeV}$ ,  $\mu/(1 + \Delta_b) = -600 \text{ GeV}$ .

## 4 $\Delta F = 2$ processes

In this section, we consider  $B_d$ ,  $B_s$ , and  $K$  mixing. We show that the enhanced effects of the renormalized quark-squark-gluino vertices vanish for degenerate squark masses. However, if the squarks are non-degenerate our (N)NLO corrections are even dominant in a large region of the parameter space. In this analysis we consider complex  $\delta_{ij}^{dAB}$ 's to exploit the data on CP asymmetries. The effective Hamiltonian is given by

$$\begin{aligned}
 H_{\text{eff}}^{\text{SUSY}} = & \frac{-\alpha_s^2}{216} \left[ V_{s23}^{dLL} V_{t23}^{dLL} \left[ 24m_{\tilde{g}}^2 D_0(m_{\tilde{d}_s}, m_{\tilde{d}_t}, m_{\tilde{g}}, m_{\tilde{g}}) + 66D_2(m_{\tilde{d}_s}, m_{\tilde{d}_t}, m_{\tilde{g}}, m_{\tilde{g}}) \right] Q_1 \right. \\
 & + V_{s23}^{dRR} V_{t23}^{dRR} \left[ 24m_{\tilde{g}}^2 D_0(m_{\tilde{d}_s}, m_{\tilde{d}_t}, m_{\tilde{g}}, m_{\tilde{g}}) + 66D_2(m_{\tilde{d}_s}, m_{\tilde{d}_t}, m_{\tilde{g}}, m_{\tilde{g}}) \right] \tilde{Q}_1 \\
 & + V_{s23}^{dLL} V_{t23}^{dRR} \left[ 504m_{\tilde{g}}^2 D_0(m_{\tilde{d}_s}, m_{\tilde{d}_t}, m_{\tilde{g}}, m_{\tilde{g}}) Q_4 - 72D_2(m_{\tilde{d}_s}, m_{\tilde{d}_t}, m_{\tilde{g}}, m_{\tilde{g}}) Q_4 \right. \\
 & \quad \left. + 24m_{\tilde{g}}^2 D_0(m_{\tilde{d}_s}, m_{\tilde{d}_t}, m_{\tilde{g}}, m_{\tilde{g}}) Q_5 + 120D_2(m_{\tilde{d}_s}, m_{\tilde{d}_t}, m_{\tilde{g}}, m_{\tilde{g}}) Q_5 \right] \\
 & + V_{s23}^{dLR} V_{t23}^{dLR} \left[ 204m_{\tilde{g}}^2 D_0(m_{\tilde{d}_s}, m_{\tilde{d}_t}, m_{\tilde{g}}, m_{\tilde{g}}) Q_2 - 36m_{\tilde{g}}^2 D_0(m_{\tilde{d}_s}, m_{\tilde{d}_t}, m_{\tilde{g}}, m_{\tilde{g}}) Q_3 \right] \\
 & \left. + V_{s23}^{dLR} V_{t23}^{dRL} \left[ -132D_2(m_{\tilde{d}_s}, m_{\tilde{d}_t}, m_{\tilde{g}}, m_{\tilde{g}}) Q_4 - 180D_2(m_{\tilde{d}_s}, m_{\tilde{d}_t}, m_{\tilde{g}}, m_{\tilde{g}}) Q_5 \right] \right]. \quad (9)
 \end{aligned}$$

For definiteness we have quoted Eq. (9) for  $B_s$  mixing but the translation to other processes is trivial. The definitions of the operators can be found in Ref. [13, 16, 18], for the remaining ingredients we follow Ref. [22] as usual.  $s$  and  $t$  label the squark mass eigenstates and a sum over  $s, t$  from 1 to 6 is understood. In the limit of two mass insertions and degenerate squark masses equation Eq. (9) simplifies to the result of [16] by substituting

$$\begin{aligned}
 D_{0,2}(m_{\tilde{q}_s}, m_{\tilde{q}_t}, m_{\tilde{g}}, m_{\tilde{g}}) & \rightarrow F_{0,2}(m_{\tilde{q}}, m_{\tilde{q}}, m_{\tilde{q}}, m_{\tilde{q}}, m_{\tilde{g}}, m_{\tilde{g}}) \\
 V_{sfi}^{qLL} & \rightarrow m_{\tilde{q}}^2 \delta_{fi}^{dLL}, \quad V_{sfi}^{qRR} \rightarrow m_{\tilde{q}}^2 \delta_{fi}^{qRR}, \quad V_{sfi}^{qRL} \rightarrow m_{\tilde{q}}^2 \delta_{fi}^{qRL}, \quad V_{sfi}^{qLR} \rightarrow m_{\tilde{q}}^2 \delta_{fi}^{qLR}. \quad (10)
 \end{aligned}$$

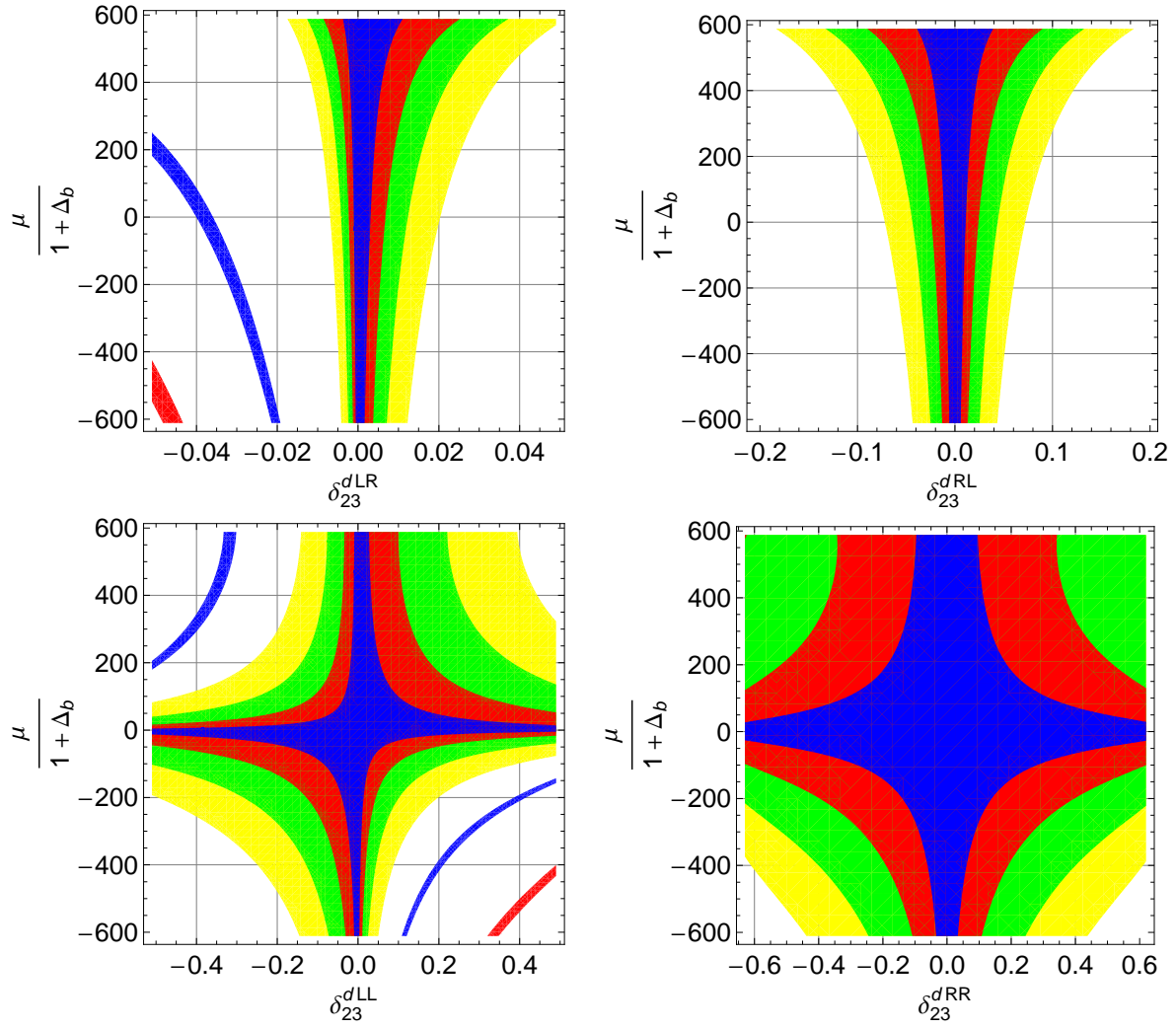


Figure 5:  $B \rightarrow X_s \gamma$ : allowed regions in the  $\delta_{23}^{dLR,RL} - \frac{\mu}{1+\Delta_b}$  and  $\delta_{23}^{dLL,RR} - \frac{\mu}{1+\Delta_b}$  planes for  $m_{\tilde{q}1,2} = 2m_{\tilde{q}3} = 1000$  GeV and  $\tan \beta = 50$ . Yellow:  $m_{\tilde{g}} = 2000$  GeV, green:  $m_{\tilde{g}} = 1500$  GeV, red:  $m_{\tilde{g}} = 1000$  GeV, blue:  $m_{\tilde{g}} = 500$  GeV (light to dark).

Eq. (9) agrees with the result in Ref. [36] and corrects two color factors in Eq. II.9 of Ref. [9]. In Ref. [20], a NLO calculation of the effective  $\Delta F = 2$  Hamiltonian has been carried out. The authors reduce the theoretical uncertainty and find corrections of about 15 percent to the LO result. They miss our effects from the flavor-changing self-energies, because they work with degenerate squark masses, so that the self-energy contributions cancel as discussed at the end of Sect. 2. As we will see, including the renormalized vertices can yield an effect of 1000% and more. So it is sufficient for our purpose to stick to the LO Hamiltonian of Eq. (9) with the renormalized vertices of Sect. 9. To incorporate the large logarithms from QCD we use the RG evolution computed in Refs. [16, 37]. For the bag factors parameterizing the hadronic matrix elements we take the lattice QCD values of Ref. [38]. We show the effects of the renormalization of the squark-quark-gluino vertex on  $\Delta M_{d,s}$  and the general pattern of the new contributions in the following subsection.

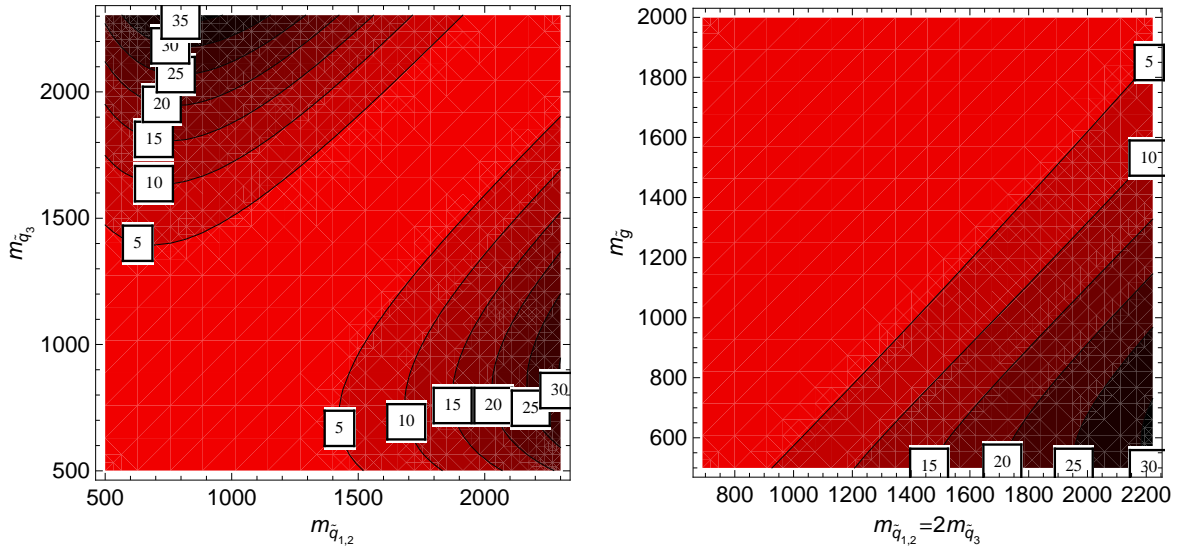


Figure 6: Left: Contour plot of  $\Delta M_{q,\text{ren}}/\Delta M_{q,\text{LO}}$  as a function of  $m_{\tilde{q}_{1,2}}$  and  $m_{\tilde{q}_3}$  with  $m_{\tilde{g}} = 1000$  GeV. Right:  $\Delta M_{q,\text{ren}}/\Delta M_{B\text{LO}}$  as a function of  $m_{\tilde{q}_{1,2}} = 2m_{\tilde{q}_3}$  and  $m_{\tilde{g}}$ . The numbers in the little squares denote the value of  $\Delta M_{q,\text{ren}}/\Delta M_{q,\text{LO}}$  of the corresponding contour.

#### 4.1 $B - \bar{B}$ mixing

The amplitude of  $B_q - \bar{B}_q$  mixing,  $q = d$  or  $s$ , is conventionally denoted by  $M_{12}$ . New physics contributions will typically change magnitude and phase of this amplitude.  $|M_{12}|$  is probed through the mass difference  $\Delta M_q$  among the two mass eigenstates of the  $B - \bar{B}$  system, while any new contribution to  $\arg M_{12}$  will modify certain CP asymmetries. For the formalism and phenomenology of  $B - \bar{B}$  mixing we refer to Ref. [39], an update of the SM contributions to  $B - \bar{B}$  mixing can be found in Ref. [40].

The chirally enhanced contributions are important for the constraints on  $\delta_{ij}^{dLR} = \delta_{ji}^{dRL*}$ . They are also relevant if one seeks constraints on  $\delta_{ij}^{dLL}$  in the large- $\tan \beta$  region, but for this case  $\text{Br}[B \rightarrow X_s \gamma]$  is more powerful. Therefore we restrict our discussion in this section to the LR elements, for which our new effects lead to drastic changes in the SUSY-contributions to  $\Delta M_q$ . We denote the result with renormalized squark-quark-gluino vertices by  $\Delta M_{q,\text{ren}}$ . In Fig. 6 we show the ratio of  $\Delta M_{q,\text{ren}}$  to the LO result  $\Delta M_{q,\text{LO}}$ , which is calculated from the gluino-squark box diagram without our new contributions. As one can easily see, the effects from the finite vertex renormalization drop out for degenerate squark masses, while dramatic effects for large and unequal squark masses are observed: For instance, a value of  $\Delta M_{q,\text{ren}}/\Delta M_{q,\text{LO}} = 50$  implies that the constraint on the studied  $\delta_{ij}^{dAB}$  is stronger by a factor of  $\sqrt{50} \approx 7$ , because both  $\Delta M_{q,\text{ren}}$  and  $\Delta M_{q,\text{LO}}$  are practically quadratic in  $\delta_{ij}^{dAB}$  (cf. MIA to see this). We remark that the value of  $\tan \beta$  is inessential in this section, varying  $\tan \beta$  leads to  $\mathcal{O}(1\%)$  changes of our  $\Delta F = 2$  results.

In order to determine the possible size of new physics (NP), it is necessary to know the SM contribution to the process in question. For  $B - \bar{B}$  mixing, this first requires the control over hadronic uncertainties, which presently obscure the quantification of NP contributions from the precise data on  $\Delta M_d$  [34] and  $\Delta M_s$  [41, 42]. In the case of  $B_d - \bar{B}_d$  mixing one must also address  $V_{td}$ , because

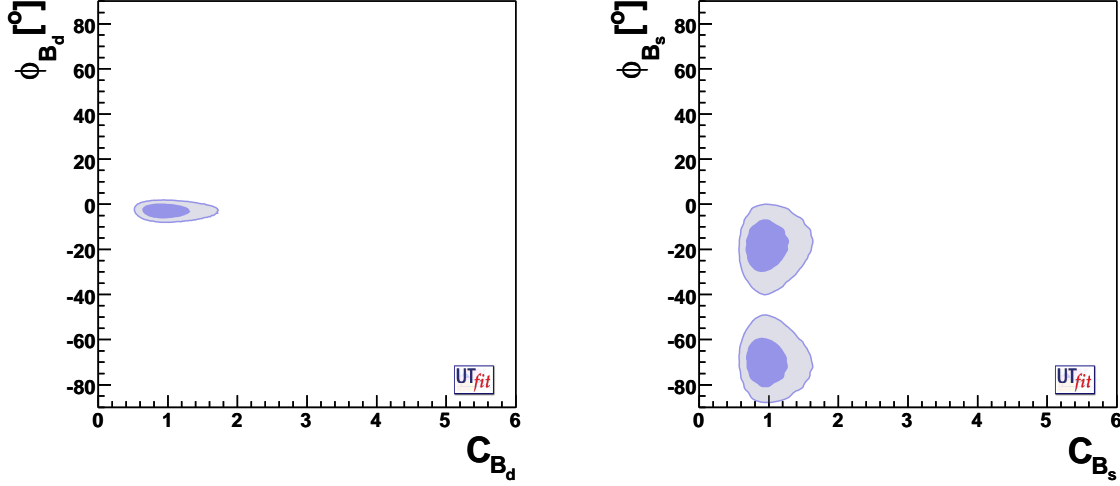


Figure 7: Allowed range for NP-contributions to  $B_q - \bar{B}_q$  mixing,  $q = d, s$ , in the  $\phi_{B_q} - C_{B_q}$  plane taken from the web update of Ref. [47]. See Eq. (11) and related text for details. For a related CKMfitter analysis see Ref. [48].

$B_d - \bar{B}_d$  mixing is used to determine this CKM element through the usual fit to the unitarity triangle. A first analysis combining different quantities probing the  $B_s - \bar{B}_s$  mixing amplitude has revealed a  $2\sigma$  discrepancy of  $\arg M_{12}$  with the SM prediction [40]. Since then the CKMfitter [43] and UTfit collaborations [44] have constrained the possible contributions of new physics to the  $B_d - \bar{B}_d$  mixing and  $B_s - \bar{B}_s$  mixing amplitudes with sophisticated statistical (Frequentist and Bayesian, respectively) methods, using new information on  $\arg M_{12}$  gained from tagged  $B_s \rightarrow J/\psi\phi$  data [45, 46]. We use the corresponding recent UTfit analysis as shown in Fig. 7. The quantities  $C_{B_q}$  and  $\phi_{B_q}$  shown in the plots are defined as:

$$C_{B_q} e^{2i\phi_{B_q}} = \Delta_q = \frac{\langle B_q | H_{\text{eff}} | \bar{B}_q \rangle}{\langle B_q | H_{\text{eff}}^{\text{SM}} | \bar{B}_q \rangle} = \frac{M_{12}}{M_{12}^{\text{SM}}} = \frac{|M_{12}^{\text{SM}}| + |M_{12}^{\text{NP}}| e^{2i\phi_{\text{NP}}}}{|M_{12}^{\text{SM}}|} \quad (11)$$

Here  $\phi_{\text{NP}}$  is the difference between the phase of the new physics contribution  $M_{12}^{\text{NP}}$  and the phase of the SM box diagrams. Refs. [40] and [48] show the experimental constraints in the complex  $\Delta_q$  planes instead. The plots in Fig. 8 show the allowed regions in the complex  $\delta_{23}^{dLR}$  and  $\delta_{13}^{dLR}$  planes. The analogous constraints on the complex  $\delta_{23}^{dRL}$  and  $\delta_{13}^{dRL}$  planes look identical, because  $|\Delta F| = 2$  processes are parity-invariant. To obtain Fig. 8 we have parameterized the border of the 95% CL region in Fig. 7 and determined the values  $\text{Re}[\delta_{13,23}^{\text{dAB}}]$  and  $\text{Im}[\delta_{13,23}^{\text{dAB}}]$  which correspond to this region by using Eq. (11) with  $M_{12}^{\text{NP}}$  calculated from  $H_{\text{eff}}^{\text{SUSY}}$  in Eq. (9). The hadronic matrix elements are conventionally expressed in terms of the product of the squared decay constant  $f_{B_q}^2$  and a bag factor. The dependence on  $f_{B_q}$  drops out in the ratio defining  $C_{B_q} e^{2i\phi_{B_q}}$ , which only involves the ratios of the bag factors of the different operators. That is, the sizable uncertainty of  $f_{B_q}$  does not enter at this step, but entirely resides in the allowed region for  $C_{B_q} e^{2i\phi_{B_q}}$  plotted in Fig. 7. Therefore our results in Fig. 8 correspond to the ranges for  $f_{B_q} \sqrt{B_q}$  (where  $B_q$  is the bag factor of the SM operator) used in (the web update of) Ref. [47]. These ranges are  $f_{B_s} \sqrt{B_s} = (270 \pm 30) \text{ MeV}$  and  $f_{B_s} \sqrt{B_s} / (f_{B_d} \sqrt{B_d}) = 1.21 \pm 0.04$  (both at  $1\sigma$ ). In the case of  $B_s - \bar{B}_s$  mixing the colored regions corresponding to different gluino masses do not overlap and do not contain the point  $\delta_{23}^{dLR} = 0$ ,

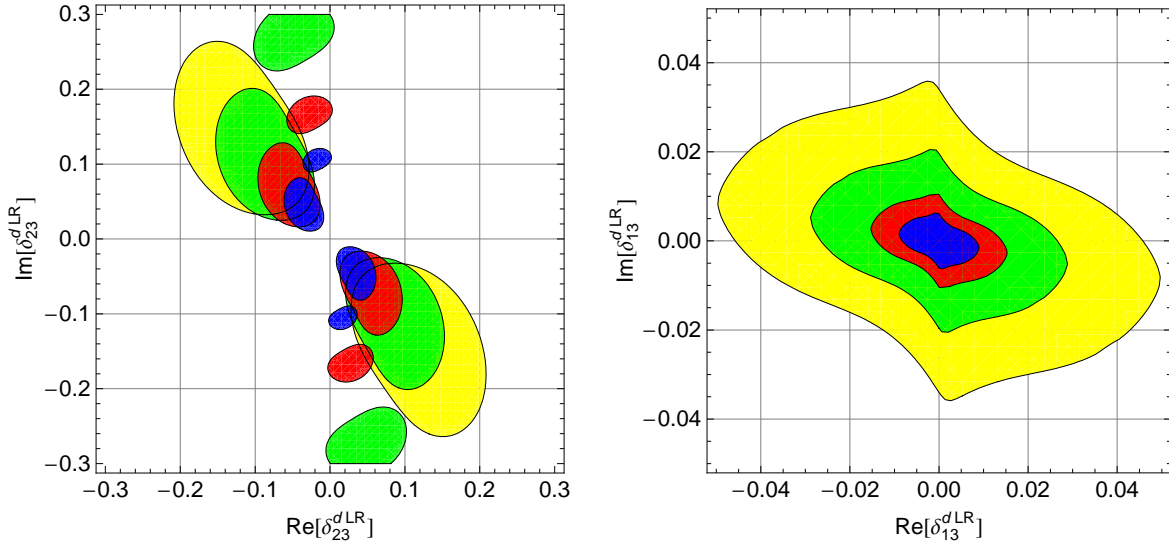


Figure 8: Allowed regions in the complex  $\delta_{13,23}^{dLR}$ -plane from  $B_s$ -mixing (left plot) and  $B_d$ -mixing (right plot) with  $m_{\tilde{q}1,2} = 2m_{\tilde{q}3} = 1000$  GeV. The yellow, green, red and blue (light to dark) areas correspond to the 95% CL regions for  $m_{\tilde{g}} = 1200$  GeV,  $m_{\tilde{g}} = 1000$  GeV,  $m_{\tilde{g}} = 800$  GeV,  $m_{\tilde{g}} = 600$  GeV. The effect is practically insensitive to  $\tan\beta$ . The same constraints are obtained for the complex  $\delta_{13,23}^{dRL}$ -plane.

because the SM value  $M_{12}^{\text{SM}}$  is not in the 95% CL region of the UFit analysis. The tension with the SM largely originates from the  $B_s \rightarrow J/\psi\phi$  data [45, 46]. A large gluino mass suppresses the supersymmetric contribution to  $M_{12}$ , so that a larger value of  $\text{Im } \delta_{23}^{dLR}$  is needed to bring  $\arg M_{12}$  into the 95% CL region.

## 4.2 $K - \bar{K}$ mixing

In  $K - \bar{K}$  mixing the situation is very different from  $B - \bar{B}$  mixing, because the chiral enhancement factor  $A_{12}^d/m_s$  involves the small  $m_s$  rather than  $m_b$ . The observed smallness of FCNC transitions among the first two generations not only forbids large  $\delta_{12}^{qAB}$  elements but also constrains the splittings among the squark masses of the first two generations severely. This observation suggests the presence of a  $U(2)$  symmetry governing the flavor structure of the first two (s)quark generations. This symmetry cannot be exact, as it is at least broken by the difference  $Y^s - Y^d$  of Yukawa couplings. That is, the numerical size of flavor- $U(2)$  breaking is somewhere between  $10^{-4}$  and a few times  $10^{-2}$ , depending on the size of  $\tan\beta$ . We may therefore fathom deviations from flavor universality in the same ballpark in the squark sector. Counting  $\Sigma_{12}^{dRL}$  as first-order in some  $U(2)$ -breaking parameter, we realize that our chiral enhancement factors are of zeroth order in  $U(2)$  breaking due to the appearance of the factor  $1/m_s$  in Eq. (5). Therefore  $K - \bar{K}$  mixing is extremely sensitive to the remaining source of flavor- $U(2)$  breaking in the problem, the mass splitting  $m_{\tilde{q}2} - m_{\tilde{q}1}$ . At this point we mention that it is important to control the renormalization of  $m_s$  in the presence of ordinary QCD corrections. In Appendix B of Ref. [30] it has been shown that all QCD corrections combine in such a way that the inverse power of  $m_s$  is the  $\overline{\text{MS}}$  mass evaluated at the scale  $Q = M_{\text{SUSY}}$ , provided that gluonic QCD corrections to  $\Sigma_{12}^{dRL}$  are also calculated in the  $\overline{\text{MS}}$  scheme.



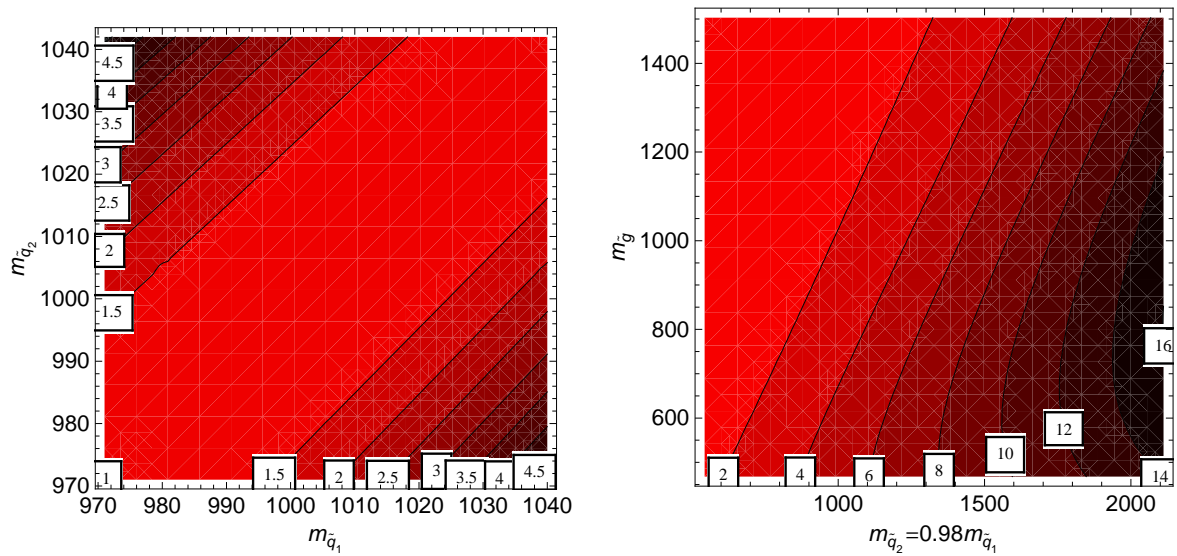


Figure 9: Left: Contour plot of  $\Delta M_{K\text{ren}}/\Delta M_{K\text{LO}}$  as a function of  $m_{\tilde{q}1}$  and  $m_{\tilde{q}2}$  with  $m_{\tilde{g}} = 1000$  GeV. Right:  $\Delta M_{K\text{ren}}/\Delta M_{K\text{LO}}$  as a function of  $m_{\tilde{q}2} = 0.98m_{\tilde{q}1}$  and  $m_{\tilde{g}}$ .

The sensitivity of the chirally enhanced corrections to the squark-mass splitting is displayed in Fig. 9. Constraints on  $\delta_{12}^{dAB}$  from  $K - \bar{K}$  mixing have been considered for a long time (see Refs. [10, 13]). Again we use the UTfit analysis (cf. the left plot of Fig. 10) exploiting the mass difference  $\Delta M_K$  and the CP-violating quantity  $\epsilon_K$ . We show our improved constraints on the complex  $\delta_{12}^{dLR}$  element in the right plot of Fig. 10. Figs. 9 and 10 are analogous to Figs. 6–8 addressing  $B - \bar{B}$  mixing; we refer to the corresponding figure captions for further explanation. We find that  $K - \bar{K}$  mixing indeed probes flavor violation in the squark sector of the first two generations at the per-mille level. The constraints on  $\delta_{12}^{dLR}$  sharply grow with  $|m_{\tilde{q}2} - m_{\tilde{q}1}|$ .

## 5 Conclusions

In the generic MSSM FCNC processes proceed through gluino-squark loop diagrams. In the present paper we have pointed out that these processes receive chirally enhanced corrections which contribute to the FCNC processes via two-loop or three-loop diagrams but can numerically dominate over the usual LO one-loop diagrams. The chirally enhanced contributions involve a flavor change in a self-energy sub-diagram attached to an external leg of the diagram. These effects can be absorbed into a finite renormalization of the squark-quark-gluino vertex. Our new effects vanish if the squark masses are degenerate. Their relative importance with respect to the LO diagrams is further larger for heavier squarks. We have consistently diagonalized the squark mass matrices exactly, thereby avoiding the mass insertion approximation. In this way the left-right mixing of bottom squarks is included correctly and the large- $\tan \beta$  region can be accessed.

Our first phenomenological study addresses  $B \rightarrow X_s \gamma$ . In this process our new effects are only relevant if  $|\mu| \tan \beta$  is large. Taking  $\tan \beta = 50$  we present new bounds on the four quantities  $\delta_{23}^{dLL}$ ,  $\delta_{23}^{dLR}$ ,  $\delta_{23}^{dRL}$ , and  $\delta_{23}^{dRR}$  which parameterize the off-diagonal elements of the down-squark mass matrix linking strange and bottom squarks. These bounds are depicted in Fig. 5 for the case of real MSSM

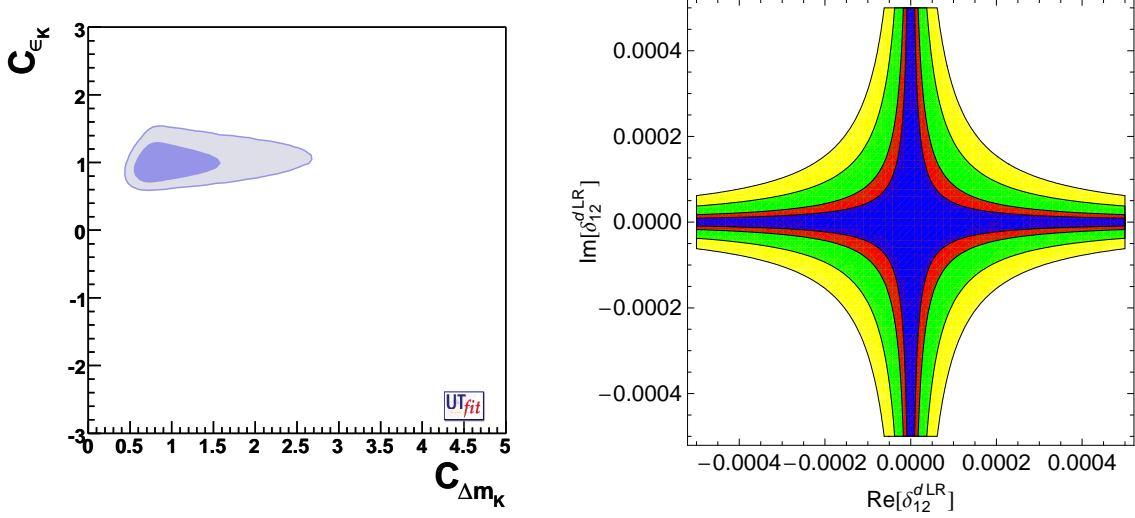


Figure 10: Left: Allowed range for NP contributions to K mixing determined by the UTfit collaboration [44]. The light region corresponds to 95% CL. Right: Allowed region in the complex  $\delta_{12}^{dLR}$ -plane with  $m_{\tilde{g}} = 750$  GeV,  $m_{\tilde{q}1} = 1000$  GeV. Yellow:  $m_{\tilde{q}2} = 1000$  GeV, green:  $m_{\tilde{q}2} = 999$  GeV, red:  $m_{\tilde{q}2} = 998$  GeV, blue:  $m_{\tilde{q}2} = 997$  GeV (light to dark). The same constraints are found for  $\delta_{12}^{dRL}$ .

parameters. As a general pattern we find that the chirally enhanced contributions decrease the size of the SUSY contribution to  $\text{Br}[B \rightarrow X_s \gamma]$  if  $\mu$  is positive. Conversely, the chirally enhanced two-loop contributions increase the SUSY contribution to  $\delta_{23}^{dAB}$  for  $\mu < 0$ . That is, for positive values of  $\mu$ , which are preferred by the anomalous magnetic moment of the muon, the bounds on  $\delta_{23}^{dAB}$  become weaker. A reduced sensitivity of  $\text{Br}[B \rightarrow X_s \gamma]$  to  $\delta_{23}^{dAB}$  is welcome for models in which the Yukawa couplings of the first two generations are zero at tree-level and light quark masses and all off-diagonal CKM elements are generated radiatively from the soft SUSY-breaking terms [22, 31]. In Ref. [22] it has been shown that this idea complies with present-day data on FCNC processes. With the weaker bound on  $\delta_{23}^{dLR}$ , which is needed to generate  $V_{cb}$ , therefore a larger portion of the MSSM parameter space becomes compatible with the radiative generation of flavor.

The second analysis of this paper is devoted to  $B_d$ ,  $B_s$ , and  $K$  mixing. Using the data on the mass differences  $\Delta M_d$  and  $\Delta M_s$  and on CP asymmetries we find new constraints on the complex  $\delta_{13}^{dLR}$ ,  $\delta_{23}^{dLR}$ ,  $\delta_{13}^{dRL}$ , and  $\delta_{23}^{dRL}$  elements (see Fig. 8). In most of the parameter space the constraints become much stronger compared to the LO analysis if the sbottom mass differs sizably from the squark masses of the first two generations, irrespective of the size of  $\tan \beta$ .  $K - \bar{K}$  mixing is even more sensitive to the chirally enhanced self-energies, provided there is a non-zero mass splitting among the squarks of the first two generations. As illustrated in Fig. 10 already mass splittings in the sub-percent range strengthen the bounds on  $\delta_{12}^{dLR}$  and  $\delta_{12}^{dRL}$  severely.

After completion of the presented work, a complete NLO calculation of supersymmetric QCD corrections to  $\Delta F = 2$  Wilson coefficients with exact diagonalization of the squark mass matrices and non-degenerate squark masses has appeared [49]. However, our chirally enhanced effects are not included, because Ref. [49] adopts the definition of the super-CKM basis based on an on-shell definition of the quark fields, as described in our Sect. 2 after Eq. (5)). With this definition the chirally enhanced effects are implicitly contained in the numerical values of the  $\delta_{ij}^{qAB}$ . While the NLO corrections of

Ref. [49] are typically numerically much smaller than ours, they are important to control the scale and scheme dependences of the LO diagrams. Therefore our results in Sect. 4 and those of Ref. [49] are complementary to each other.

## Acknowledgments

The authors thank Lars Hofer and Dominik Scherer for many fruitful discussions and Javier Virto for e-mail exchange about the renormalization of the squark-quark-gluino vertex. We further thank the referee for drawing our attention to Ref. [21]. This work is supported by BMBF under grant no. 05H09VKF and by the EU Contract no. MRTN-CT-2006-035482, “FLAVIANet”. Andreas Crivellin acknowledges the financial support of the State of Baden-Württemberg through *Strukturiertes Promotionskolleg “Elementarteilchenphysik und Astroteilchenphysik”*.

## References

- [1] S. Dimopoulos and H. Georgi, Nucl. Phys. B **193** (1981) 150.
- [2] J. R. Ellis and D. V. Nanopoulos, Phys. Lett. B **110** (1982) 44.
- [3] R. Barbieri and R. Gatto, Phys. Lett. B **110** (1982) 211.
- [4] M. J. Duncan, Nucl. Phys. B **221** (1983) 285.
- [5] J. F. Donoghue, H. P. Nilles and D. Wyler, Phys. Lett. B **128** (1983) 55.
- [6] L. J. Hall, V. A. Kostelecky and S. Raby, Nucl. Phys. B **267** (1986) 415.
- [7] F. Gabbiani and A. Masiero, Nucl. Phys. B **322** (1989) 235.
- [8] S. Bertolini, F. Borzumati, A. Masiero and G. Ridolfi, Nucl. Phys. B **353** (1991) 591.
- [9] J. S. Hagelin, S. Kelley and T. Tanaka, Nucl. Phys. B **415** (1994) 293.
- [10] F. Gabbiani, E. Gabrielli, A. Masiero and L. Silvestrini, Nucl. Phys. B **477** (1996) 321 [arXiv:hep-ph/9604387].
- [11] J. A. Bagger, K. T. Matchev and R. J. Zhang, Phys. Lett. B **412** (1997) 77 [arXiv:hep-ph/9707225].
- [12] M. Ciuchini, E. Franco, V. Lubicz, G. Martinelli, I. Scimemi and L. Silvestrini, Nucl. Phys. B **523** (1998) 501 [arXiv:hep-ph/9711402].
- [13] M. Ciuchini *et al.*, JHEP **9810** (1998) 008 [arXiv:hep-ph/9808328].
- [14] F. Borzumati, C. Greub, T. Hurth and D. Wyler, Phys. Rev. D **62** (2000) 075005 [arXiv:hep-ph/9911245].
- [15] T. Besmer, C. Greub and T. Hurth, Nucl. Phys. B **609** (2001) 359 [arXiv:hep-ph/0105292].

- [16] D. Becirevic *et al.*, Nucl. Phys. B **634**, 105 (2002) [arXiv:hep-ph/0112303].
- [17] M. Ciuchini, E. Franco, A. Masiero and L. Silvestrini, Phys. Rev. D **67** (2003) 075016 [Erratum-  
ibid. D **68** (2003) 079901] [arXiv:hep-ph/0212397].
- [18] M. Ciuchini and L. Silvestrini, Phys. Rev. Lett. **97** (2006) 021803 [arXiv:hep-ph/0603114].
- [19] M. Ciuchini, E. Franco, D. Guadagnoli, V. Lubicz, M. Pierini, V. Porretti and L. Silvestrini,  
Phys. Lett. B **655** (2007) 162 [arXiv:hep-ph/0703204].
- [20] M. Ciuchini, E. Franco, D. Guadagnoli, V. Lubicz, V. Porretti and L. Silvestrini, JHEP **0609**  
(2006) 013 [arXiv:hep-ph/0606197].
- [21] J. Foster, K. i. Okumura and L. Roszkowski, Phys. Lett. B **609** (2005) 102  
[arXiv:hep-ph/0410323].  
J. Foster, K. i. Okumura and L. Roszkowski, JHEP **0508** (2005) 094 [arXiv:hep-ph/0506146].  
J. Foster, K. i. Okumura and L. Roszkowski, JHEP **0603** (2006) 044 [arXiv:hep-ph/0510422].  
J. Foster, K. i. Okumura and L. Roszkowski, Phys. Lett. B **641** (2006) 452  
[arXiv:hep-ph/0604121].
- [22] A. Crivellin and U. Nierste, Phys. Rev. D **79**, 035018 (2009) [arXiv:0810.1613 [hep-ph]].  
A. Crivellin, arXiv:0905.3130 [hep-ph].
- [23] A. Crivellin, arXiv:0907.2461 [hep-ph].
- [24] T. Banks, Nucl. Phys. B **303** (1988) 172.
- [25] L. J. Hall, R. Rattazzi and U. Sarid, Phys. Rev. D **50** (1994) 7048 [arXiv:hep-ph/9306309].  
M. S. Carena, M. Olechowski, S. Pokorski and C. E. M. Wagner, Nucl. Phys. B **426** (1994) 269  
[arXiv:hep-ph/9402253].
- [26] C. Hamzaoui, M. Pospelov and M. Toharia, Phys. Rev. D **59** (1999) 095005  
[arXiv:hep-ph/9807350]. K. S. Babu and C. F. Kolda, Phys. Rev. Lett. **84** (2000) 228  
[arXiv:hep-ph/9909476].
- [27] A. J. Buras, P. H. Chankowski, J. Rosiek and L. Slawianowska, Nucl. Phys. B **619**  
(2001) 434 [arXiv:hep-ph/0107048]. G. Isidori and A. Retico, JHEP **0111** (2001) 001  
[arXiv:hep-ph/0110121]. G. D'Ambrosio, G. F. Giudice, G. Isidori and A. Strumia, Nucl. Phys.  
B **645** (2002) 155 [arXiv:hep-ph/0207036]. A. J. Buras, P. H. Chankowski, J. Rosiek and  
L. Slawianowska, Phys. Lett. B **546** (2002) 96 [arXiv:hep-ph/0207241]. A. Dedes and A. Pi-  
laftsis, Phys. Rev. D **67** (2003) 015012 [arXiv:hep-ph/0209306]. A. J. Buras, P. H. Chankowski,  
J. Rosiek and L. Slawianowska, Nucl. Phys. B **659** (2003) 3 [arXiv:hep-ph/0210145]. M. Gor-  
bahn, S. Jager, U. Nierste and S. Trine, arXiv:0901.2065 [hep-ph].
- [28] M. S. Carena, D. Garcia, U. Nierste and C. E. M. Wagner, Nucl. Phys. B **577**, 88 (2000)  
[arXiv:hep-ph/9912516].
- [29] S. Marchetti, S. Mertens, U. Nierste and D. Stockinger, Phys. Rev. D **79** (2009) 013010  
[arXiv:0808.1530 [hep-ph]].
- [30] L. Hofer, U. Nierste and D. Scherer, JHEP **0910** (2009) 081 [arXiv:0907.5408 [hep-ph]].

- [31] F. Borzumati, G. R. Farrar, N. Polonsky and S. D. Thomas, arXiv:hep-ph/9805314. F. Borzumati, G. R. Farrar, N. Polonsky and S. D. Thomas, Nucl. Phys. B **555** (1999) 53 [arXiv:hep-ph/9902443]. J. Ferrandis and N. Haba, Phys. Rev. D **70**, 055003 (2004) [arXiv:hep-ph/0404077].
- [32] H. E. Logan and U. Nierste, Nucl. Phys. B **586** (2000) 39 [hep-ph/0004139].
- [33] G. Degrandi, P. Gambino, and P. Slavich, Phys. Lett. B **635** (2006) 335 [hep-ph/0601135].
- [34] C. Amsler *et al.* [Particle Data Group], Phys. Lett. B **667** (2008) 1.
- [35] M. Misiak and M. Steinhauser, Nucl. Phys. B **764** (2007) 62 [arXiv:hep-ph/0609241].
- [36] S. Baek, T. Goto, Y. Okada and K. i. Okumura, Phys. Rev. D **64** (2001) 095001 [arXiv:hep-ph/0104146].
- [37] A. J. Buras, S. Jager and J. Urban, Nucl. Phys. B **605** (2001) 600 [arXiv:hep-ph/0102316].
- [38] V. Lubicz and C. Tarantino, Nuovo Cim. **123B** (2008) 674 [arXiv:0807.4605 [hep-lat]].
- [39] K. Anikeev *et al.*, *B physics at the Tevatron: Run II and beyond*, [hep-ph/0201071]. U. Nierste, *Three Lectures on Meson Mixing and CKM phenomenology*, arXiv:0904.1869 [hep-ph].
- [40] A. Lenz and U. Nierste, JHEP **0706** (2007) 072 [arXiv:hep-ph/0612167].
- [41] A. Abulencia *et al.* [CDF Collaboration], Phys. Rev. Lett. **97** (2006) 242003 [arXiv:hep-ex/0609040].
- [42] V. M. Abazov *et al.* [DØ Collaboration], Phys. Rev. Lett. **98** (2007) 151801 [arXiv:hep-ex/0701007].
- [43] J. Charles *et al.* [CKMfitter Group], Eur. Phys. J. C **41** (2005) 1 [arXiv:hep-ph/0406184] updated results and plots available at: <http://ckmfitter.in2p3.fr>.
- [44] M. Ciuchini *et al.*, JHEP **0107** (2001) 013 [arXiv:hep-ph/0012308]. We use the updated results at <http://www.utfit.org>
- [45] T. Aaltonen *et al.* [CDF Collaboration], Phys. Rev. Lett. **100** (2008) 161802 [arXiv:0712.2397 [hep-ex]]. T. Aaltonen *et al.* [CDF Collaboration], “An updated Measurement of the CP violating phase  $\beta_s^{J/\psi\phi}$ ,” CDF public note 9458.
- [46] V. M. Abazov *et al.* [DØ Collaboration], Phys. Rev. Lett. **101** (2008) 241801 [arXiv:0802.2255 [hep-ex]].
- [47] M. Bona *et al.* [UTfit Collaboration], arXiv:0803.0659 [hep-ph]. Fig. 7 taken from update at <http://www.utfit.org>.
- [48] V. Tisserand [CKMfitter Collaboration], *CKM fits as of winter 2009 and sensitivity to New Physics*, talk at *XLIVth Recontres de Moriond, Electroweak Interactions and Unified Theories*, La Thuile, Aosta Valley, Italy, 2009, arXiv:0905.1572 [hep-ph]; and work in progress.
- [49] J. Virto, JHEP **0911** (2009) 055 [arXiv:0907.5376 [hep-ph]].

